MAGNETOHYDRODYNAMICS Vol. 48 (2012), No. 1, pp. 213–220

FLOW STRUCTURES ARISING FROM MELT STIRRING BY MEANS OF MODULATED ROTATING MAGNETIC FIELDS

D. Räbiger[1], *S. Eckert*[1], *G. Gerbeth*[1], *S. Franke*[2], *J. Czarske*[2]

[1] *Helmholtz Zentrum Dresden-Rossendorf (HZDR), PO. Box 510119 – 01314 Dresden, Germany*

[2] *Technische Universitat Dresden, Helmholtzstrasse 18, 01069 Dresden, Germany*

We present an experimental study concerning measurements of the flow inside a liquid metal column exposed to a pulsed rotating magnetic field. A novel ultrasound Doppler system was used to measure two-dimensional velocity fields of the secondary flow in the radial-meridional plane. It employs an array of 25 transducer elements allowing a fast electronic traversing with concurrently high spatial and temporal resolution. The measurements revealed transient flow regimes showing distinct inertial oscillations and coherent vortex structures. The results demonstrate that the arising flow structure depends sensitively on the duration of the RMF pulses.

1. Introduction. Electromagnetic stirring during solidification has been proved to be a striking method for achieving a purposeful alteration of the microstructure of casting ingots, such as grain refinement or the promotion of a transition from a columnar to an equiaxed dendritic growth (CET). However, the imposition of a rotating (RMF) or a travelling magnetic field (TMF) also causes problems like the occurrence of a typical segregation pattern or a deflection of the upper free surface. A permanent radial inward (RMF and downward TMF) or outward (upward TMF) flow along the solidification front is responsible for the transport of solute to the axis or to the wall of the ingot resulting in a typical freckle segregation pattern filled with an overage of eutectic composition [1, 2]. Several studies have been devoted to overcoming the handicaps of rotary stirring with the specific goal to generate a vigorous stirring in the bulk without considerable deformations of the free surface [3–5]. It was shown recently that the application of modulated AC magnetic fields offers considerable potential for optimizing the melt stirring [6, 7]. Especially, the secondary flow can be organized in such a way that periodic reversals of the flow direction occur adjacent to the solidification front, which is essential to prevent flow-induced macrosegregation [8]. It has become apparent that a careful adjustment of the modulation parameters is required to create intense secondary flows with periodic reversals of the flow direction.

Within this paper, we especially consider the effect of a pulsed RMF on the isothermal liquid metal flow inside a circular cylinder, whereas the RMF is applied in form of successive rectangular pulses. Previous investigations revealed the existence of an optimal pulse length T_{P}, where a maximum intensity of a periodic meridional flow was observed [7]. In that case, the corresponding pulse frequency f_{P} is related to the eigenperiod of inertial waves in a developed regime, as given by Greenspan [9]. The present study is aimed at highly resolved, quantitative velocity measurements in order to disclose the flow pattern resulting from various modulated driving forces differing with respect to the respective pulse length.

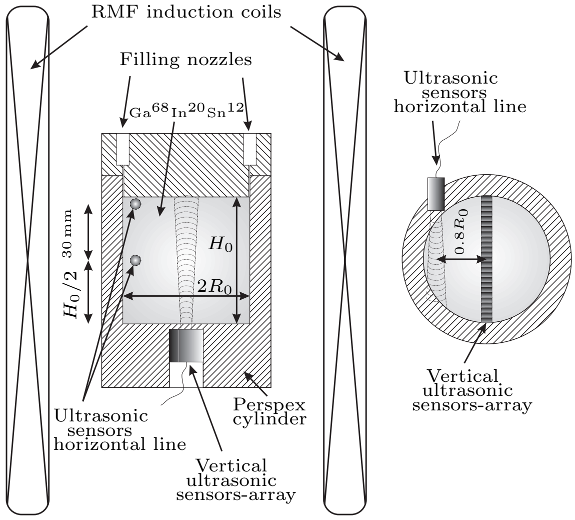

Fig. 1. Schematic view of the experimental setup.

2. Experimental setup. A schematic view of the experimental setup is shown in Fig. 1. A cylindrical vessel made of Plexiglas was used with an aspect ratio $A = H_0/(2R_0) = 1$. The size of the inner diameter $D = 2R_0$ and height H_0 was chosen to be 67.5 mm. The cylinder is closed by rigid lids and filled with the eutectic alloy GaInSn. The experiments were performed in the magnetic induction system PERM at HZDR, wherein the fluid vessel was placed concentrically. In order to preclude flow artefacts arising from symmetry deviations of the experimental setup (vertical alignment, conformity of both the cylinder and the magnetic field axis), special care was necessary to ensure a precise positioning of the cylinder inside the magnetic system. The homogeneity of the magnetic field was checked using a 3-axis Gauss meter (Lakeshore model 560, sensor type MMZ2560-UH). Within a radius of 35 mm, which approximately corresponded to the radial dimension of the container, the variance of the magnetic field strength was found to be smaller than 3%.

The ultrasound Doppler velocimetry (UDV) was used to perform measurements of the fluid flow inside the cylinder. Details with respect to the measuring principle can be found in [10]. The DOP2000 velocimeter (model 2125, Signal Processing SA, Lausanne) equipped with a 4 MHz transducer (TR0405LS, acoustic active diameter 5 mm) was applied to measure the primary azimuthal flow at two vertical positions. By attaching the ultrasonic transducer to the wall of the fluid container, the acoustic coupling between the sensor and the fluid was realized through the curved cylindrical surface. Moreover, a flow mapping of the meridional flow was carried out by using a new measuring system operating with a linear array of 25 single transducers attached to the plane-parallel bottom wall of the flow container (see Fig. 1). Details of the measuring system are given in [11]. The spatial resolution in lateral direction varies from 5 mm at the sensor to approximately 7.5 mm at the lid of the fluid vessel. In the axial direction, a spatial resolution of about 1.4 mm was achieved. The velocity data were acquired with sampling frequencies between 0.5 and 6 Hz. The accuracy of the velocity data can be assessed to be better than 0.15 mm/s.

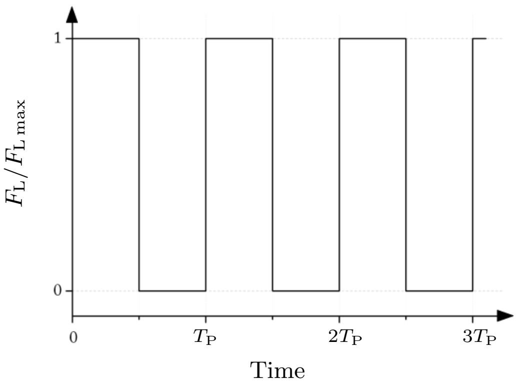

Fig. 2. Modulation scheme of the driving Lorentz force F_L.

3. Results. The modulation scheme of the pulsed RMF as considered within this study is displayed in Fig. 2. As a consequence, the fluid flow experiences a sequence of spin-up and spin-down processes. The duration of the particular pulse cycles T_P turns out to be a crucial control parameter. Measurements of both the primary and the secondary flow have been carried out for different values of T_P. Figs. 3,4 shows time series of the mean vertical velocity and local azimuthal velocity u_φ for three different pulse durations. Here, the vertical velocity u_z in Fig. 3 has been averaged across the vertical mid-plane of the cylinder as follows:

$$\bar{u} = \frac{1}{H_0 R_0^2} \int_{H_0/2}^{H_0} \int_{-R_0}^{R_0} r\sqrt{u_z^2}\,\mathrm{d}r\mathrm{d}z. \tag{1}$$

After a transient behaviour related to the initiation of the electromagnetic driving force, the measurements reveal a distinct periodicity of both the primary and the

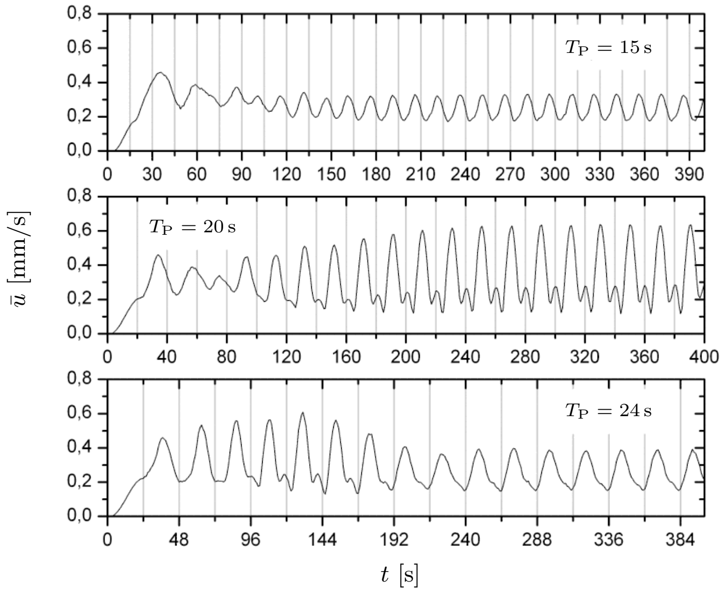

Fig. 3. Time-resolved measurements of the vertical velocity ($B_{RMF} = 0.46$ mT).

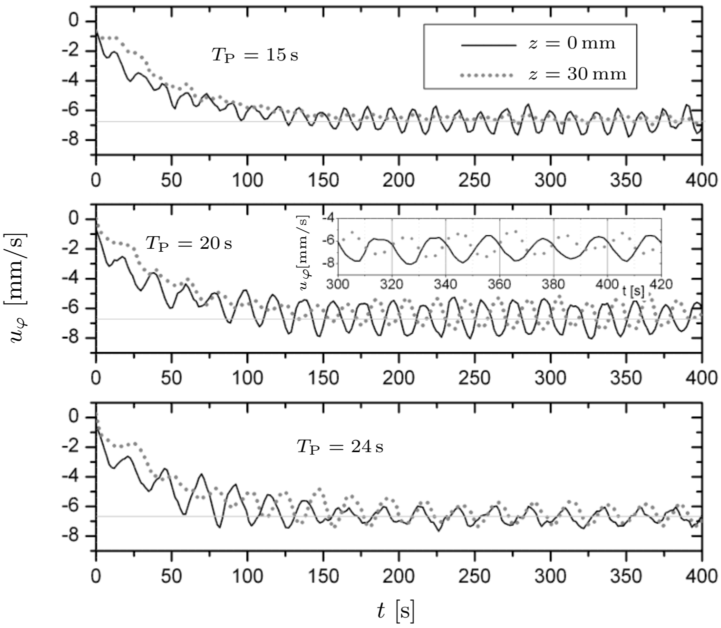

Fig. 4. Time-resolved measurements of the azimuthal velocity ($B_{\mathrm{RMF}} = 0.46$ mT).

secondary flow, whereas the cycle duration corresponds to the particular pulse cycle T_P. The rising edges of a particular RMF pulse appear as gray branch lines in the diagrams. While the flow oscillations appear to be very regular for a pulsing at $T_\mathrm{P} = 15$ s (Fig. 3), the oscillation amplitude of the secondary flow increases significantly for $T_\mathrm{P} = 20$ s. More precisely, a doubling of the frequency occurs with respect to $1/T_\mathrm{P}$ and every second peaks becomes very intense. This phenomenon, which disappears again with the further increase of the pulse cycle, is similar to a resonant circuit. Another indication can be noticed in Fig. 4, where the azimuthal velocity is recorded at two different vertical positions. These two curves exhibit a distinct phase shift for $T_\mathrm{P} = 20$ s.

Fig. 5 shows two snapshots of the flow pattern obtained for a pulse cycle of $T_\mathrm{P} = 20$ s. The typical structure of the toroidal double vortex can be detected in Fig. 5*a*. The secondary flow in the central region is directed upwards in the bottom part and downwards in the upper part of the cylinder, respectively. The moment when this double vortex appears coincides with the large peak of the secondary flow in Fig. 3. The smaller peak of $\bar{u}$ corresponds to the snapshot shown in Fig. 5*b*. Here, we can observe an inversion of the flow direction, the so-called “inverse” double vortex is formed at lower intensity.

The mean values of the vertical velocity averaged over both the total measuring time and the vertical cylinder cross-section are presented in Fig. 6 vs. the pulse duration cycle T_P for a magnetic field strength of 0.46 mT. It becomes obvious that the intensity of the secondary flow exhibits a pronounced maximum around $T_\mathrm{P} \approx 20$ s, where distinct periodic reversals of the secondary flow were observed. This resonance peak is shifted to a lower T_P with the increasing magnetic field strength as depicted in Fig. 7, in particular, the maximum is found at $T_\mathrm{P} = 2.9$ s for $B_{\mathrm{RMF}} = 2.25$ mT. Moreover, further maxima of the magnitude of the averaged secondary flow appear at larger pulse durations.

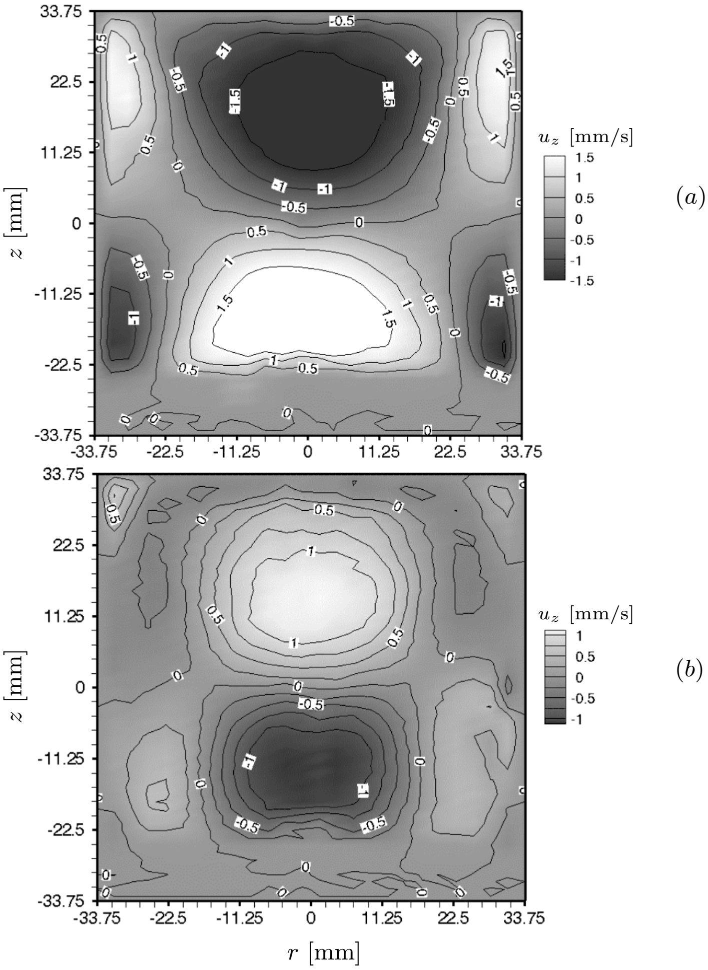

Fig. 5. Snapshots of the vertical velocity across the vertical mid-plane of the cylinder recorded by the US sensor array for $T_{\mathrm{P}} = 20\,\mathrm{s}$ at $B_{\mathrm{RMF}} = 0.46\,\mathrm{mT}$: (*a*) typical double vortex of the secondary flow; (*b*) "inverse" double vortex.

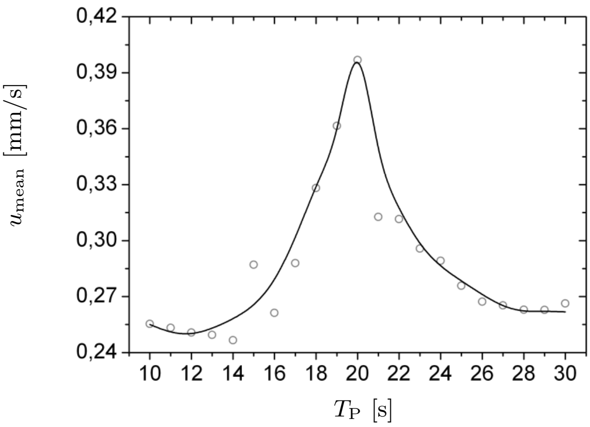

Fig. 6. Dependence of the secondary flow intensity on the duration of the pulse cycle T_{P}: $B_{\mathrm{RMF}} = 0.46\,\mathrm{mT}$.

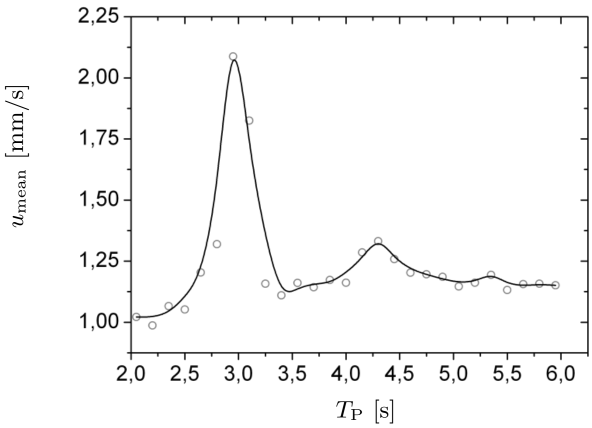

Fig. 7. Dependence of the secondary flow intensity on the duration of the pulse cycle T_{P}: $B_{\text{RMF}} = 2.25\,\text{mT}$.

Fig. 8 presents snapshots of the vertical flow obtained for pulse durations of $T_{\text{P}} = 4.3\,\text{s}$ and $5.3\,\text{s}$, respectively, which correspond to the second and third peak in Fig. 7. It is interesting to note that a new flow pattern emerges marked by an increment of vortex cells in the radial direction.

4. Discussion and conclusions. The present study concerns a liquid metal flow, being exposed to a pulsed RMF. The alternating power up and power down of the magnetic field generates successive spin-ups and spin-downs of the rotating fluid flow. Abrupt changes in energy injection rates promote the propagation of inertial waves through the interior of the fluid [12, 13]. Such waves were derived for the case of small perturbations to a fluid, which rotates as a solid body [9]. Because the Coriolis force balances the pressure gradients and generates the restoring force for the inertial waves, their wavelengths and frequencies are related in a special way. The theoretically determined eigenperiod (of the inertial waves was given by Greenspan [9]:

$$\tau = \frac{\pi}{\Omega}\left[1 + \left(\frac{\gamma_i}{n\pi}\right)^2 \left(\frac{H_0}{R_0}\right)^2\right]^{1/2} \tag{2}$$

where γ_i denotes the i-th root of the Bessel function $J_1(x)$ (for reference, $\gamma_1 = 3.832$, $\gamma_2 = 7.016$, $\gamma_3 = 10.174$). The angular rotation rate Ω has been determined from our measurements. Considering the axisymmetric inertial mode $k = 0$, $n = 2$, $m = 1$, we obtain eigenperiods of $20.6\,\text{s}$ and $3.1\,\text{s}$ for magnetic field intensities of $0.46\,\text{mT}$ and $2.25\,\text{mT}$, respectively. These results agree very well with the experimentally identified T_{P} values for the respective main resonance peaks. The parameter region around these resonance frequencies of the driving force appears as optimal working regions for an efficient electromagnetic stirring, because the intensity of the secondary flow reaches a distinct maximum here. Moreover, the permanent reversals of the flow direction make this flow regime promising for applications in directional solidification processes. The electromagnetic control of the flow direction prevents a unidirectional transport of solute along the solidification front and, hence, allows to avoid the formation of flow-induced segregation channels.

A prolongation of the pulse duration T_{P} at $2.25\,\text{mT}$ produces minor maxima of the magnitude of the secondary flow. Using Eq. (2), we yield eigenperiods of

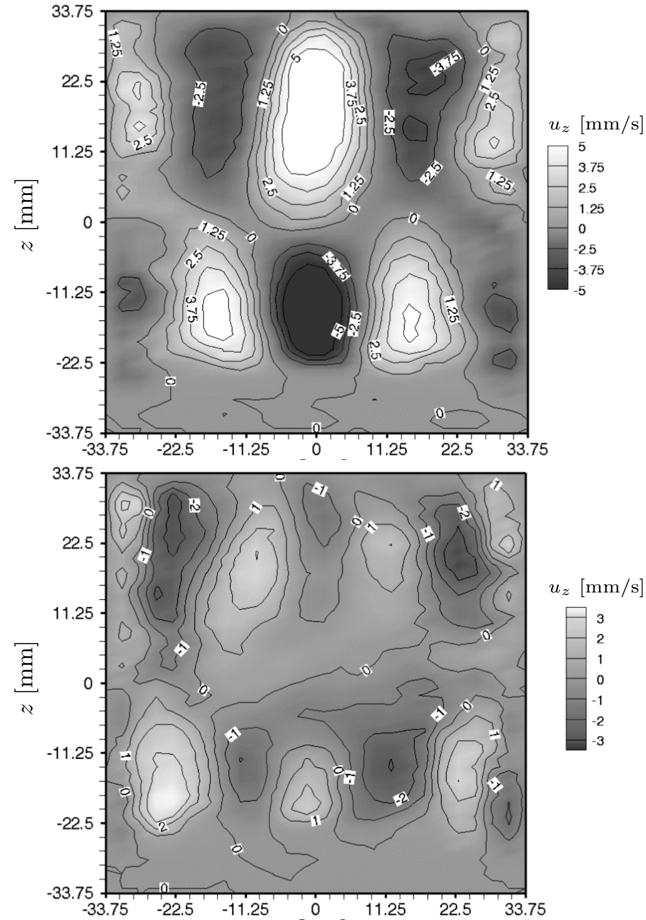

Fig. 8. Snapshots of the vertical velocity across the vertical mid-plane of the cylinder recorded by the US sensor array at $B_{\mathrm{RMF}} = 2.25\,\mathrm{mT}$: (*a*) $T_{\mathrm{P}} = 4.3\,\mathrm{s}$; (*b*) $T_{\mathrm{P}} = 5.3\,\mathrm{s}$.

4.6 s and 6.4 s, which correspond fairly well to the minor peaks in Fig. 7. These higher modes manifest themselves in a new secondary flow pattern showing an incremented number of vortex cells in the radial direction.

The electromagnetic stirring method, which uses a modulated RMF, offers considerable potential to enhance the stirring efficiency and optimize the properties of castings by a well-aimed flow control during solidification. Further investigations are necessary to improve the understanding of the development of various flow regimes under the influence of a time-modulated driving force.

Acknowledgements. The research is supported by the Deutsche Forschungsgemeinschaft (DFG) in form of the SFB 609 "Electromagnetic Flow Control in Metallurgy, Crystal Growth and Electrochemistry".

REFERENCES

[1] M. Medina, Y. Du Terrail, F. Durand, Y. Fautrell. *Metall. Mater. Trans. B*, vol. 35B (2004), pp. 743–755.

[2] P. Nikrityuk, K. Eckert, R. Grundmann. *Int. J. Heat Mass Transfer*, vol. 49 (2006), pp. 1501–1511.

[3] C. Vives. *Metall. Trans. B*, vol. 24B (1993), pp. 493–510.

[4] S. Taniguchi, K. Mataike, M. Okubo, T. Ando, K. Ueno. *Proc. of the 4th Int. Conf. on Electromagnetic Processing of Materials (EPM)* (Sendai, 2003), pp. 339–343.

[5] K.-H. Spitzer, G. Reiter, K. Schwerdtfeger. *ISIJ Int.*, vol. 6 (1996), pp. 487–492.

[6] S. Kojima, T. Ohnishi, T. Mori, K. Shiwaku, I. Wakasugi, M. Ohgarni. *Proc. of the 66th Steelmaking Conf.* (Atlanta, 1983), pp. 127–131.

[7] S. Eckert, P. Nikrityuk, D. Räbiger, K. Eckert, G. Gerbeth. *Metall. Mater. Trans. B*, vol. 38B (2007), pp. 977–988.

[8] B. Willers, S. Eckert, P. Nikrityuk, D. Räbiger, J. Dong, K. Eckert, G. Gerbeth. *Metall. Mater. Trans. B*, vol. 39B (2008), pp. 304–316.

[9] H.P. Greenspan. *The theory of rotating fluids* (Breukelen Press, Brookline, 1990).

[10] Y. Takeda. *Nucl. Eng. Design*, vol. 126 (1991), pp. 277–284.

[11] S. Franke, L. Büttner, J. Czarske, D. Räbiger, S. Eckert. *Flow Meas. Instrum.*, vol. 21 (2010), pp. 402–409.

[12] P. Nikrityuk, M. Ungarish, K. Eckert, R. Grundmann. *Phys. Fluids*, vol. 17 (2005), p. 067101.

[13] D. Räbiger, S. Eckert, G. Gerbeth. *Exp. Fluids*, vol. 48 (2010), pp. 233–244.

Received 16.02.2012